CrossMark

Ancient stardust in fine-grained chondrule dust rims from carbonaceous chondrites

Jan Leitner [a,*], Christian Vollmer [b], Christine Floss [c], Jutta Zipfel [d], Peter Hoppe [a]

[a] *Max Planck Institute for Chemistry, Particle Chemistry Department, Hahn-Meitner-Weg 1, 55128 Mainz, Germany*
[b] *Institute for Mineralogy, Westfälische Wilhelms-Universität, Correnstrasse 24, 48149 Münster, Germany*
[c] *Laboratory for Space Sciences and Physics Department, Washington University, One Brookings Drive, St. Louis, MO 63130, USA*
[d] *Forschungsinstitut und Naturmuseum Senckenberg, Sektion Meteoritenforschung, Senckenberganlage 25, 60325 Frankfurt, Germany*

ARTICLE INFO

ABSTRACT

Carbonaceous chondrites are fragments from primitive parent asteroids, which represent some of the most primitive meteorites accessible for laboratory analysis and offer therefore the best opportunity to explore the chemical and physical conditions in the early Solar System. Here, we report the identification of presolar grains, which are circumstellar condensates that date back from before the formation of our Solar System, in fine-grained dust rims around chondrules in carbonaceous chondrites. Average presolar grain abundances in the rims of aqueously altered chondrites (petrologic type 2) are three times higher than in the respective interchondrule matrices, while for the most pristine specimens (petrologic type 3), the opposite is observed. The presence of these grains implies a nebular origin of the rim material, and gives evidence for differing alteration pathways for different reservoirs of fine-grained material found in primitive meteorites. Moreover, our findings indicate formation of the fine-grained rims in the solar nebula prior to parent-body accretion, giving support to accretionary scenarios for parent-bodies in the presence of dust-rimmed chondrules.

© 2015 Elsevier B.V. All rights reserved.

1. Introduction

Primitive meteorites, interplanetary dust particles (IDPs), and cometary matter contain small but significant amounts of refractory dust grains with highly anomalous isotopic compositions. The observed isotopic anomalies cannot be explained by chemical or physical processes occurring in the solar system, but are the result of nucleosynthetic reactions in stellar environments. These grains formed in the winds of evolved stars and in the ejecta of stellar explosions, were incorporated in the protosolar nebula and survived alteration and homogenization processes during the formation of the solar system. They represent samples of ancient stardust available for laboratory analysis (e.g., Zinner, 2014). Investigation of the isotopic compositions and mineralogies of these grains provides valuable information on stellar nucleosynthesis and evolution, grain growth in circumstellar environments, the types of stars that contributed material to our planetary system, and chemical and physical processes in the interstellar medium and in the early Solar System. Moreover, parent body (i.e., asteroidal) alter-

ation processes can be studied by using presolar grain abundances as tracers, as is the case for the present study.

Refractory silicates are the most abundant presolar grain type, if nanodiamonds, whose abundances and origins are a matter of ongoing discussion, are neglected (Zinner, 2014). Matrix-normalized abundances depend on the degree of secondary alteration experienced by the host material, but can exceed 200 ppm in the most primitive meteorites (e.g., Nguyen et al., 2007; Floss and Stadermann, 2009; Vollmer et al., 2009a; Nittler et al., 2013). Presolar oxides are somewhat less abundant, with abundances of up to tens of ppm in meteorites (e.g., Vollmer et al., 2009a; Leitner et al., 2012). The majority of presolar O-rich grains are divided into four distinct groups, according to their oxygen isotopic compositions (Nittler et al., 1997, 2008). These groups reflect different stellar origins, with major contributions from low-mass red giant stars and smaller but still significant contributions from supernovae.

In past investigations, the fine-grained matrix material hosting the larger meteorite components (ICM – interchondrule matrix – hereafter) has been targeted for presolar grain searches. However, further fine-grained components are also present in primitive meteorites, such as fine-grained rims (FGR) around chondrules and fine-grained lithic clasts with distinct boundaries embedded in surrounding material. The origin and nature of fine-grained
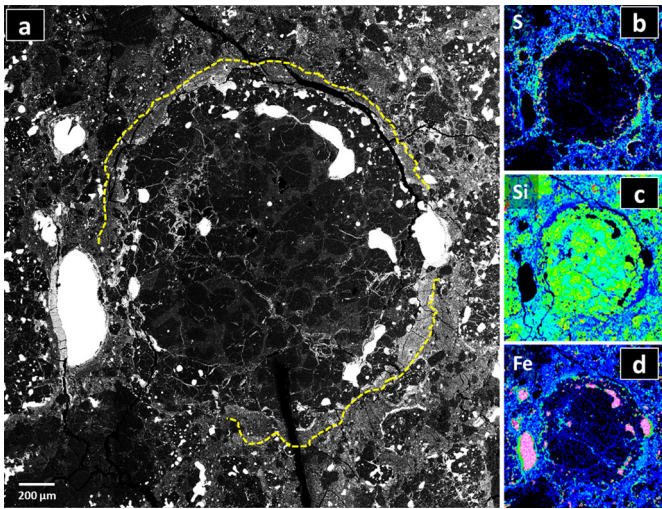
Fig. 1. (a) BSE- and X-ray elemental maps of (b) S, (c) Si and (d) Fe of a rimmed chondrule in GRA 95229. The FGR contains the presolar grains GR9513_6, GR95_13_22, GR95_13_24, GR95_13_27, GR95_13_29, and GR95_14_13 (Table 2). The dashed yellow line in panel (a) marks the outline of the FGR, which can also be identified from the elemental maps in (b–d). (For interpretation of the references to color in this figure legend, the reader is referred to the web version of this article.)

rims around chondrules has been and is still discussed controversially. Both nebular (e.g., Allen et al., 1980; Metzler et al., 1992; Ciesla et al., 2003; Chizmadia and Brearley, 2008; Bland et al., 2011) and parent body (e.g., Sears et al., 1993; Tomeoka and Tanimura, 2000; Trigo-Rodriguez et al., 2006) formation processes have been suggested, based on a wide variety of observations. If the FGRs accreted in a nebular setting, relatively pristine material like stardust grains or isotopically anomalous organic material could have been preserved there, possibly modified by parent body alteration. Parent body scenarios include chondrule erosion or accretion in the regolith. However, not all structures described as "fine-grained rims" are alike. The FGRs studied in this paper (Fig. 1, Table S1), as well as those investigated in CO (Davidson, 2009; Haenecour and Floss, 2012; Davidson et al., 2012; Haenecour et al., 2014) and CM chondrites (e.g., Metzler et al., 1992; Chizmadia and Brearley, 2008; Leitner et al., 2013) share certain properties like the co-existence of primitive, nearly unaltered components with constituents that have undergone aqueous alteration, on small scales (micrometer to sub-micrometer range). In contrast, the rims described by Tomeoka and Tanimura (2000) and Takayama and Tomeoka (2012) in several CV chondrites and the Tagish Lake meteorite, have been affected heavily by aqueous alteration and may well have a different origin.

The CR (Renazzo-type) group of carbonaceous chondrites is considered to be among the most primitive meteorites (Krot et al., 2002). They exhibit bulk ^{15}N enrichments with δ^{15}N between +20‰ and +230‰ (depending on weathering grade and state of alteration), hosted in isotopically anomalous organic matter found in these meteorites. Individual isotopic hotspots display ^{15}N enrichments of up to a factor of three (Busemann et al., 2006; Alexander et al., 2007). The degree of aqueous alteration observed within the CR group varies from heavily altered to very little alteration. There is an ongoing debate whether the least altered CR chondrites (MET 00426, QUE 99177) are of petrologic type 2 or 3; however, recently found evidence for aqueous alteration (Le Guillou and Brearley, 2014) would speak against a classification as type 3. A more sensitive scale for the degree of aqueous alteration experienced by CR chondrites is desirable, since such information would ultimately allow differences in the presolar grain abundances due to differing degrees of alteration to be disentangled from inherent heterogeneities. Several approaches have been undertaken to establish more refined

classification schemes (Alexander et al., 2013; Harju et al., 2014; Howard et al., 2015). However, these approaches have not yet provided a petrological classification that reflects the vast differences in presolar grain abundances and distributions observed for the CR chondrites (Fig. S2). For more extensively altered meteorites, the scale devised by Harju et al. (2014) is consistent with the significantly lower presolar silicate and oxide abundances observed for Renazzo. However, Alexander et al. (2013) assigned a subtype to Renazzo which puts it in line with the most pristine CR chondrites, indicating less aqueous metamorphism than in QUE 99177. Similar problems are encountered with the scheme by Howard et al. (2015). Here, MET 00426 is assigned 2.6, while QUE 99177, GRA 95229 and even GRA 06100 are classified as 2.8. There are several possible explanations for this apparent discrepancy. First of all, heterogeneous alteration within the CRs might be an important issue. Second, variations of the alteration temperatures could have affected the fraction of surviving presolar silicates and oxides (Alexander et al., 2013). Finally, TEM studies have found that the amorphous silicates in the minimally altered CR chondrite MET 00426 contain water (Le Guillou and Brearley, 2014). These authors ascribe their findings to the simultaneous accretion of dust and ice. The latter produced localized centers of aqueous alteration on sublimation, offering an explanation for the survival of larger amounts of presolar grains in MET 00426 than in the CR2 chondrites (which therefore might have experienced alteration at higher temperatures).

Bulk O-isotopic data for the fine-grained matrix of a set of CR chondrites (Schrader et al., 2014) seem to correlate quite well with both the degree of alteration of the respective meteorite and the abundances of presolar O-anomalous grains from the current study (Fig. S3). However, there is (yet) only small overlap between the sample sets, and heterogeneous alteration also has to be taken into account, as can be seen from differing results for individual samples from the same specimen. Therefore, we refrained from adopting any of these classification schemes for the meteorites studied here.

Early studies of CR chondrites indicated only low presolar O-anomalous dust abundances (Nagashima et al., 2004; Floss and Stadermann, 2005). However, more recent investigations (Floss and Stadermann, 2009; Leitner et al., 2012; Nguyen et al., 2010; Zhao et al., 2013) have revealed much higher oxygen-rich presolar dust concentrations in several of these meteorites. CR chondrites offer the opportunity to study the effects of alteration on primitive meteoritic material from a common reservoir in the early solar nebula. It has been suggested that the range of presolar silicate concentrations among different meteorites is due to secondary alteration processes (e.g., Floss and Stadermann, 2009), which destroy presolar silicate grains preferentially over more refractory presolar phases such as oxides or carbonaceous grains, as has been earlier discussed by Huss et al. (2003).

Here, we report the identification of oxygen-rich presolar grains in fine-grained chondrule rims of several CR chondrites, as well as the ungrouped carbonaceous chondrite Acfer 094. The presence of stardust, together with other primitive materials, indicates a nebular origin of the fine-grained material of which the chondrule rims are comprised. Moreover, formation of these rims must have occurred prior to the formation of the respective meteorite parent bodies. Thus, our findings give strong support to nebular formation scenarios.

2. Materials and methods/experimental

2.1. Sample characterization

All investigated samples (Table 1) were characterized by backscatter electron (BSE) imaging and X-ray elemental mapping with

Table 1

Samples and sizes of analyzed areas investigated in this study.

Meteorite	Source	Sample no.	FGR area (μm^2)^2/no. of studied FGRs	ICM area (μm^2)	Shock stage
Acfer 094 (C3-ungr.)	NHM Vienna	M5928	3500/2	–	S1[a]
EET 92161 (CR2)	NASA JSC	17	6500/1	4600	
GRA 95229 (CR2)	NASA JSC	97	7200/2	5700	S1[b]
MET 00426 (CR3)	NASA JSC	13	5600/1	5900	S2[b]
MIL 07525 (CR2)	NASA JSC	09	4800/2	4600	S2[b]
NWA 801 (CR2)	NHM London	P11648	2600/1	1800	
Renazzo (CR2)	NHM Vienna	A437/L3812	12,200/3	6500	S1–S3[c]

[a] Newton et al. (1995).
[b] Harju et al. (2014).
[c] Scott et al. (1992).

a LEO 1530 Field Emission Scanning Electron Microscope (FE-SEM) equipped with an Oxford INCA/Aztec EDS system at the Max Planck Institute for Chemistry (MPIC). Additional element distribution maps were acquired with a JEOL Superprobe 8200 Electron Microprobe at the MPI for Chemistry. Rim structures were identified either from BSE images or X-ray element maps (see Fig. 1 for an example).

2.2. Isotopic measurements by NanoSIMS

Suitable regions of these fine-grained materials were selected for analysis of O-isotopic compositions with the NanoSIMS 50 ion probe at the MPIC in Mainz. In addition, C and N isotopes were measured on a subset of fine-grained material (one FGR in GRA 95229, one FGR in EET 92161, and interchondrule matrix areas in GRA 95229). All isotope measurements were performed by ion imaging with a primary Cs^+ beam (100 nm diameter, $\sim$1 pA) which was rastered over 10×10 μm^2-sized sample areas. For a more detailed description of applied data reduction and correction procedures see Leitner et al. (2012). Prior to analysis, the carbon coating was removed from sample areas of 14×14 μm^2 in size by sputtering with a high current primary beam ($\sim$20 pA). Oxygen and subsequent C, N analyses were then performed within these areas with the "chained analysis" setup, i.e., after defining a starting position, measurements are carried out automatically, with the sample stage moving in a predefined pattern to subsequent areas. To identify O-anomalous signatures, secondary ion images of $^{16}O^-$, $^{17}O^-$, $^{18}O^-$, $^{28}Si^-$, and $^{27}Al^{16}O^-$ were acquired in multi-collection mode. Each individual measurement consisted of 4–5 image planes of 11 min integration time each over 10×10 μm^2 areas (256×256 pixels). Presolar silicate and oxide grains were identified by their anomalous O-isotopic composition, and detection of $^{28}Si^-$ and $^{27}Al^{16}O^-$ allowed an initial distinction between silicates and Al-rich oxides. A grain was considered presolar if its O-isotopic composition differs by at least 4σ from that of the surrounding matrix. The measured O-isotopic compositions of presolar grains were normalized to O-rich material in the surrounding matrix, which was assumed to have solar system isotopic ratios. Presolar grain abundances were calculated by dividing the visible area of all grains in a certain area (determined either from the isotopic ratio images or, if available, from high-resolution SEM images) by the total scanned area. Additionally, $^{12}C^-$, $^{13}C^-$, $^{12}C^{14}N^-$, $^{12}C^{15}N^-$, and $^{28}Si^-$ were measured in multi-collection mode to determine the N-isotopic composition of organic material in several FGR and ICM regions. During these measurements, 4–5 image planes of 11 min integration time each were acquired over 10×10 μm^2-sized areas (256×256 pixels). Nitrogen isotopic ratios were normalized to those measured on a synthetic N-doped SiC-standard. All obtained data were processed with in-house software developed at the MPIC.

2.3. Auger electron spectroscopy (AES)

The elemental compositions of presolar silicate grains in the two CR2 chondrites GRA 95229 and EET 92161 were analyzed with the PHI 700 Auger Nanoprobe at Washington University in St. Louis, using established procedures for presolar silicate grains (Stadermann et al., 2009). Briefly, Auger electron energy spectra are obtained with a 10 kV 0.25 nA primary electron beam, which is rastered over the grains of interest, allowing the determination of the elemental compositions with a lateral resolution of 10–20 nm. Multiple spectral scans of a given grain are added together to obtain a single Auger spectrum, which is acquired in 1 eV steps and then subjected to a 7-point Savitsky–Golay smoothing and differentiation routine prior to peak identification and quantification. Sensitivity factors for the major rock-forming elements (O, Si, Fe, Mg, Ca, and Al) were determined from olivine and pyroxene standards of various compositions.

2.4. SEM-FIB/TEM analysis of FGR material

A total of 4 lamellae from 3 FGRs were prepared with the "focused ion beam" (FIB) technique (e.g., Wirth, 2004; Zega et al., 2007). With the FEI Nova 600 Nanolab Dual-Beam FIB Workstation at the Max Planck Institute for Polymer Research (MPIP) in Mainz, thin ($\sim$100–150 nm) slices for subsequent Transmission electron microscopy (TEM) analyses were produced. TEM analyses were performed on a Zeiss Libra 200FE (200 kV) at the Institute for Mineralogy at the University of Münster for bright field (BF) imaging, selected area electron diffraction (SAED), EDS measurements, and scanning TEM-high angle annular dark field (HAADF) images. X-ray counts were collected for $\sim$100 s using an ultra-thin window Noran spectrometer, to obtain a relative counting statistical error of $<$10%. The spectra were quantified using standard background corrections and Cliff-Lorimer thin-film criteria, the detection limit for major elements with these settings is $\sim$0.5 at.%.

3. Results and discussion

3.1. Identification of presolar silicate and oxide grains in rims and matrix

We investigated a total of 9 fine-grained chondrule rims in 5 moderately to extensively altered CR2 chondrites (1 in EET 92161, 2 in GRA 95229, 2 in MIL 07525, 1 in NWA 801, 3 in Renazzo), together with selected interchondrule matrix regions in each meteorite by NanoSIMS ion imaging. A total area of 57,600 μm^2 of fine-grained material was scanned (33,300 μm^2 of FGRs, 1100 μm^2 of fine-grained lithic clast material, and 23,200 μm^2 of ICM), and 43 presolar O-rich grains were identified (39 silicates and 4 Al-rich oxides, Table 2). The majority (33) of these grains (30 silicates, 3 Al-oxides) are located in fine-grained rims (corresponding to a
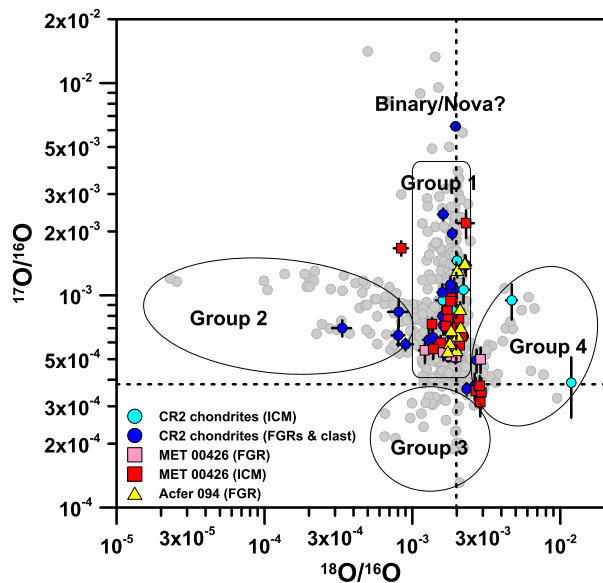
Fig. 2. Oxygen-isotopic ratios of presolar O-anomalous grains (silicates and oxides) identified in FGRs and one matrix-like clast (blue symbols) as well as in the ICM of the five CR chondrites investigated in this study. Grain groups (Nittler et al., 1997, 2008) are symbolized by ellipses. For comparison, data for presolar silicates and oxides (gray symbols) from Bland et al. (2007), Bose et al. (2010, 2012), Choi et al. (1998), Floss and Stadermann (2009, 2012), Leitner et al. (2012), Mostefaoui and Hoppe (2004), Nagashima et al. (2004), Nguyen et al. (2007, 2010), Nittler et al. (1997, 2008), Vollmer et al. (2009a, 2009b), Zhao et al. (2013), and Zinner et al. (2003) are plotted. Errors are 1σ. The solar system average ratios are indicated by the dashed lines. (For interpretation of the references to color in this figure legend, the reader is referred to the web version of this article.)

grain density of 990 ± 170 mm^{-2} in the FGRs). One presolar silicate was found in a fine-grained lithic clast, while 9 O-anomalous grains (8 silicates, 1 Al-oxide) were found in the "classical" interchondrule matrix, representing a grain density of 390 ± 130 mm^{-2} in the ICM (Table 2, Fig. 2).

In addition to the moderately to extensively altered CR2 chondrites, we also studied one FGR (5600 µm^2) and a similar-sized ICM area (5900 µm^2) in the minimally altered CR2 chondrite MET 00426, together with two FGRs in the C-ungrouped chondrite Acfer 094 (3550 µm^2). The rim areas in Acfer 094 contained 9 presolar silicates (according to a grain density of 2500 ± 850 mm^{-2}), while the MET FGR and ICM contained 6 presolar O-anomalous grains (five silicates and one Al-rich oxide grain) and 19 presolar silicate grains, respectively (Table 3, Fig. 2), corresponding to grain densities of 1070 ± 440 mm^{-2} and 3220 ± 740 mm^{-2}.

3.2. Presolar grain abundances

The 43 O-anomalous grains in the moderately to extensively altered CR2 chondrites studied here represent an overall presolar grain abundance of 45 ± 7 ppm (42 ± 7 ppm for silicates and $3(+2/-1)$ ppm for oxides). All errors are 1σ and were based on the confidence limits for small numbers according to Gehrels (1986). The majority of the presolar silicate and oxide grains were found in FGRs, with O-anomalous grain abundances that are lower by about a factor of 3 in the ICM compared to FGRs, when we calculate the "total" abundances for all studied rims and all matrix areas in all moderately to extensively altered CR2s (in order to improve counting statistics, see Fig. 3).

If we assume that the precursor material in the CR formation reservoir in the solar nebula was well-mixed, the distribution of presolar grains should have been more or less uniform. Davidson et al. (2014) investigated the abundances of presolar SiC in chondritic meteorites and found no significant variations. However, SiC

and oxygen-rich dust particles condense during different evolutionary stages of the respective parent star, thus, a comparison between the abundances of O-rich and C-rich presolar dust might not be straightforward. Nevertheless, if we adopt a uniform distribution of presolar silicates and oxides in the protosolar cloud as a first-order assumption, no significant preferential destruction of silicate stardust occurred, especially in the FGRs, emphasizing their primitive nature, with the exception of Renazzo. The lower silicate stardust concentrations in the Renazzo rims could be indicative of more severe aqueous alteration that also reduced the presolar silicate concentration in the FGRs. This observation is also supported by an average presolar O-anomalous grain abundance of 14 $(+11/-5)$ ppm for FGRs in the CM chondrites (calculated from data given in Leitner et al., 2013), which generally experienced more severe aqueous alteration than the CR chondrites (e.g., Brearley, 2006). We observe a predominance of presolar silicates over oxides for all samples, independent from the degree of alteration experienced by the host meteorite. Therefore, following the assumption that presolar silicates were preferentially destroyed by aqueous alteration, while refractory oxides were more resistant (Floss and Stadermann, 2009; Leitner et al., 2012), alteration in the CR2 chondrites was not severe enough to cause a significant difference in the presolar silicate/oxide ratios in comparison to the most pristine meteorites. Due to the overall low presolar oxide abundances and the resulting large statistical errors, no significant difference in the silicate/oxide ratios of FGRs and ICM could be observed.

For the CR chondrite MET 00426, we observe that the ICM contains $\sim$5 times more O-anomalous grains than the FGR (Fig. 3). For Acfer 094, the large error for the abundance of presolar grains in FGR material precludes a meaningful comparison. Similar trends are observed for rims and matrix in several CO3.0 chondrites (Fig. 3), with the abundance difference between ICM and FGRs attributed to more extensive aqueous alteration affecting the CO rims (Haenecour et al., 2014).

While the average abundances for FGRs and ICM in the minimally altered type 2 and the type 3 chondrites could, in principle, be attributed to more severe aqueous alteration affecting the rims than the interchondrule matrix, this explanation does not hold for the CR2 chondrites. Here, the FGRs cannot have formed by simple (parent body) aqueous alteration of fine-grained material in the vicinity of the chondrules, since this should result in even lower grain abundances than those observed in the ICM of the meteorites. Instead, a two-stage alteration model seems more plausible. First, the FGRs formed prior to chondrule incorporation into the parent body. During this period, the rim material experienced compaction to a certain degree, which also led to a reduction of the presolar grain abundances (see also section 3.5). Subsequent parent body alteration resulted in further reduced abundances in the ICM of the moderately to more severely altered CR2 chondrites, while the potential compaction experienced by the FGRs preserved more presolar grains here. Despite the low counting statistics for presolar grains especially in the ICM of individual CR2s, the calculated overall FGR and ICM grain abundances for the moderately to more severely altered CR chondrites support this interpretation.

3.3. Nitrogen isotopic composition, mineralogy, and microstructure of the rim material

The FGRs from GRA 95229, EET 92161, and Renazzo also show significant enrichments in ^{15}N (Table S2, Fig. 4). One FGR in GRA 95229 has an average δ^{15}N of $185 \pm 2‰$, similar to the N-isotopic composition of insoluble organic matter (IOM) in this meteorite (δ^{15}N $= 153 \pm 7‰$, Alexander et al., 2007). Isotopic hotspots with δ^{15}N of 500–750‰ were also found. A FGR in EET 92161 displays

Table 2

Presolar silicates and oxides identified in fine-grained chondrule rims, interchondrule matrix, and one lithic matrix clast in the CR2 chondrites of this study. "Gr." denotes the group of the respective grain (Nittler et al., 1997, 2008); "Min." gives the mineralogy of the grain (sil.: silicate, ox.: (Al-rich) oxide, com.: complex grain with oxide core and silicate rim). Grain sizes in italics were determined from ion images, all other were derived by SEM.

Meteorite	Loc.	Grain	Size (nm)	$^{17}O/^{16}O(\times 10^{-4})$	$^{18}O/^{16}O(\times 10^{-3})$	Gr.	Min.
GRA 95229	clast	GR95_04_16	490×310	5.17 ± 0.29	1.95 ± 0.06	1	sil.
GRA 95229	ICM	GR95_08_07	370×240	7.95 ± 0.76	1.80 ± 0.11	1	com.
GRA 95229	FGR	GR95_12_5	235×265	6.87 ± 0.40	1.88 ± 0.07	1	sil.
GRA 95229	FGR	GR95_12_6	250×200	5.16 ± 0.32	1.97 ± 0.06	1	sil.
GRA 95229	FGR	GR95_13_6	200×145	5.21 ± 0.27	2.01 ± 0.05	1	oxide
GRA 95229	FGR	GR95_13_22	400×130	6.96 ± 0.61	0.33 ± 0.03	2	sil.
GRA 95229	FGR	GR95_13_24	245×160	5.11 ± 0.29	1.96 ± 0.06	1	sil.
GRA 95229	FGR	GR95_13_27	580×360	6.43 ± 0.70	0.80 ± 0.08	2	sil.
GRA 95229	FGR	GR95_13_29	370×230	62.54 ± 2.51	1.96 ± 0.14	ext.1[a]	sil.
GRA 95229	FGR	GR95_14_13	400×215	8.29 ± 1.24	0.81 ± 0.12	2	sil.
Renazzo	FGR	REN_02_20	225×250	7.99 ± 0.77	1.60 ± 0.11	1	sil.
Renazzo	FGR	REN_04_06	225×425	5.96 ± 0.35	1.82 ± 0.06	1	sil.
Renazzo	FGR	REN_08_23	220×190	3.75 ± 0.53	2.64 ± 0.14	4	sil.
EET 92161	FGR	EET_2B_9	205×310	3.62 ± 0.24	2.33 ± 0.06	4	sil.
EET 92161	FGR	EET_2B_2	495×410	6.43 ± 0.57	1.84 ± 0.10	1	sil.
EET 92161	FGR	EET_02A_B_2	290×200	6.17 ± 0.80	1.29 ± 0.11	1	sil.
EET 92161	FGR	EET_02A_B_3	190×200	6.18 ± 0.37	2.04 ± 0.07	1	sil.
EET 92161	FGR	EET_02A_B_10	430×400	6.09 ± 0.34	1.90 ± 0.06	1	sil.
EET 92161	FGR	EET_02A_B_15	130×90	10.65 ± 1.40	1.92 ± 0.18	1	ox.
EET 92161	FGR	EET_02A_B_31*	334×334	7.73 ± 0.77	1.82 ± 0.12	1	sil.
EET 92161	FGR	EET_03B_5	225×310	6.43 ± 0.61	2.23 ± 0.11	1	sil.
EET 92161	ICM	EET_4_2	175×120	9.47 ± 1.29	1.61 ± 0.17	1	sil.
EET 92161	ICM	EET_5B_5	145×185	10.62 ± 1.50	2.22 ± 0.20	1	sil.
EET 92161	ICM	EET_6_6	320×220	3.87 ± 1.23	11.89 ± 0.69	4	sil.
EET 92161	ICM	EET_6_13	175×100	8.44 ± 0.87	1.88 ± 0.13	1	sil.
EET 92161	ICM	EET_6_15	310×270	9.47 ± 1.79	4.70 ± 0.40	4	sil.
EET 92161	ICM	EET_6_14*	330×330	8.62 ± 0.99	1.97 ± 0.15	1	ox.
NWA 801	FGR	NWA801_01B_7_1	300×295	24.06 ± 0.16	1.62 ± 0.13	1	sil.
NWA 801	FGR	NWA801_01B_7_2	190×150	6.23 ± 0.48	1.98 ± 0.09	1	sil.
NWA 801	FGR	NWA801_1B_9	200×135	6.77 ± 0.71	1.81 ± 0.12	1	sil.
NWA 801	FGR	NWA801_01B2_3	330×180	5.13 ± 0.28	1.75 ± 0.05	1	sil.
NWA 801	FGR	NWA801_01B3_6	400×260	5.05 ± 0.27	1.96 ± 0.05	1	sil.
MIL 07525	ICM	MIL_R4#6	385×300	14.60 ± 1.22	2.01 ± 0.14	1	sil.
MIL 07525	ICM	MIL_R4#12	430×330	7.10 ± 0.51	1.67 ± 0.08	1	sil.
MIL 07525	FGR	MIL_R3#13	535×310	19.50 ± 1.18	1.86 ± 0.12	1	sil.
MIL 07525	FGR	MIL_R2#2	170×180	10.70 ± 1.19	1.80 ± 0.16	1	sil.
MIL 07525	FGR	MIL_R2#13	255×165	13.80 ± 1.50	2.30 ± 0.20	1	sil.
MIL 07525	FGR	MIL_R2#16	200×310	4.94 ± 0.61	2.72 ± 0.14	4	sil.
MIL 07525	FGR	MIL_R8#2	270×165	10.30 ± 0.97	1.60 ± 0.12	1	sil.
MIL 07525	FGR	MIL_R8#10	265×210	11.20 ± 1.08	1.81 ± 0.14	1	sil.
MIL 07525	FGR	MIL_R8#11	290×325	7.25 ± 0.73	1.62 ± 0.11	1	sil.
MIL 07525	FGR	MIL_R9#5	280×225	5.87 ± 0.37	0.90 ± 0.11	2	ox.
MIL 07525	FGR	MIL_R9#10	320×220	6.33 ± 0.88	1.38 ± 0.12	1	sil.

[a] "Extreme" Group 1 grain; see, e.g., Vollmer et al. (2009b).

an average $\delta^{15}N$ of $55 \pm 7‰$, significantly lower than the typical ^{15}N-enrichment of CRs, but in the same range that we observe for interchondrule matrix in GRA 95229 ($\delta^{15}N65 \pm 4‰$). However, individual measurement areas in the EET rim show a wide spread of values, $\sim 0‰ < \delta^{15}N < 273‰$. Hotspots with ^{15}N-enrichments of up to $730‰$ are observed. FGRs in Renazzo have an average $\delta^{15}N$ of $\sim 107 \pm 2‰$; and one ^{15}N-rich hotspot ($730 \pm 40‰$) was detected. The presence of heavy nitrogen-bearing organics gives further evidence for the nebular origin of the rim material, as well as a common origin for the ICM and FGR material. ^{15}N-enriched insoluable organic material is commonly observed in the matrix of CR chondrites (e.g., Alexander et al., 2007). Extensive aqueous or thermal alteration would significantly affect and ultimately equilibrate the isotopic anomaly carried by these materials. The variation of the N-anomaly over individual measurement areas (Fig. 4) hints towards heterogeneous aqueous alteration.

We carried out TEM investigations on four FIB-prepared lamellae from presolar grain-bearing FGRs (two from GRA 95229, and one each from EET 92161 and MIL 07525, including the two rims containing N-anomalies) to study mineralogical textures. The FGRs in GRA 95229 consist of a complex assemblage of Fe-sulfides, anhydrous Mg-rich silicates, nearly unaltered Fe,Ni-metal grains and

phyllosilicates (serpentine), all set in a partly amorphous Fe-rich silicate groundmass. Carbonaceous matter is also present as irregular interstitial material throughout the FIB sections, partially as well-preserved nanoglobules (Fig. 5). Some fayalitic olivines are recrystallized, indicating alteration, and several Fe-sulfides display alteration rims. However, the overall texture is very similar to the fine-grained material from other primitive carbonaceous chondrites with sulfide-rich and -poor areas and a comparably high porosity, e.g., MET 00426, QUE 99177 (Abreu and Brearley, 2010), ALHA 77307 (Brearley, 1993), or Yamato 791198 (Chizmadia and Brearley, 2008). We estimate the fraction of amorphous silicates in the GRA 95229 rim roughly to be $\sim 10–20\%$. The rim material from MIL 07525 contains only a few anhydrous silicates, and even these show signs of alteration. Amorphous silicates make up $\sim 1–10\%$ of this rim. The FGR in EET 92161 shows signs of more extensive aqueous alteration and contains virtually no amorphous silicates ($<1\%$). The presence of such (at least partially) primitive assemblages with hotspots of heavy N, globular organic material and presolar dust in the FGRs supports the idea that FGRs were formed by accretion of dust and ice in the solar nebula on chondrule surfaces prior to parent body formation, as suggested by Metzler et al. (1992). No correlation was observed between the content of amor-

Table 3
Presolar silicates and oxides identified in fine-grained chondrule rims, interchondrule matrix, and one lithic matrix clast in the minimally altered chondrites studied here (MET 00426 (CR), Acfer 094 (C-ungrouped)). "Gr." denotes the group of the respective grain (Nittler et al., 1997, 2008); "Min." gives the mineralogy of the grain (sil.: silicate, ox.: (Al-rich) oxide). Grain sizes were determined from ion images.

Meteorite	Loc.	Grain	Size (nm)	$^{17}O/^{16}O(\times 10^{-4})$	$^{18}O/^{16}O(\times 10^{-3})$	Gr.	Min.
MET 00426	ICM	MET_01B_10	230 × 280	9.72 ± 1.06	1.86 ± 0.15	1	sil.
MET 00426	ICM	MET_01B_11	280 × 290	8.46 ± 0.98	1.73 ± 0.14	1	sil.
MET 00426	ICM	MET_01B_12	270 × 280	7.32 ± 0.49	1.36 ± 0.07	1	sil.
MET 00426	ICM	MET_01B_15	165 × 235	5.96 ± 0.48	1.56 ± 0.08	1	sil.
MET 00426	ICM	MET_01B_16	235 × 260	3.54 ± 0.53	2.69 ± 0.15	4	sil.
MET 00426	ICM	MET_01B_20_1	290 × 350	7.72 ± 0.76	1.74 ± 0.11	1	sil.
MET 00426	ICM	MET_01B_20_2	235 × 280	6.35 ± 0.46	2.08 ± 0.08	1	sil.
MET 00426	ICM	MET_01B_28	235 × 300	3.50 ± 0.58	2.93 ± 0.16	4	sil.
MET 00426	ICM	MET_01B_41	255 × 315	16.70 ± 1.30	0.84 ± 0.09	2	sil.
MET 00426	ICM	MET_01B_50	200 × 280	5.59 ± 0.59	1.38 ± 0.09	1	sil.
MET 00426	ICM	MET_01B_53_1	325 × 445	9.37 ± 0.84	1.81 ± 0.11	1	sil.
MET 00426	ICM	MET_01B_53_2	260 × 260	5.82 ± 0.45	2.09 ± 0.08	1	sil.
MET 00426	ICM	MET_01B_55	245 × 280	7.73 ± 0.49	2.07 ± 0.07	1	sil.
MET 00426	ICM	MET_01B_61	350 × 400	21.90 ± 0.33	2.31 ± 0.30	1	sil.
MET 00426	ICM	MET_01B_62	350 × 420	7.17 ± 0.50	1.69 ± 0.07	1	sil.
MET 00426	ICM	MET_01B_65	300 × 325	3.74 ± 0.43	2.85 ± 0.12	4	sil.
MET 00426	ICM	MET_01B_66	235 × 280	6.41 ± 0.58	2.16 ± 0.11	1	sil.
MET 00426	ICM	MET_01B_67	235 × 235	7.02 ± 0.62	2.01 ± 0.10	1	sil.
MET 00426	ICM	MET_01B_68	220 × 220	3.14 ± 0.45	2.88 ± 0.14	4	sil.
MET 00426	FGR	MET_01A_8	210 × 260	5.19 ± 0.30	1.81 ± 0.06	1	sil.
MET 00426	FGR	MET_01A_13	190 × 190	4.99 ± 0.69	2.89 ± 0.16	4	sil.
MET 00426	FGR	MET_01A_22	260 × 315	5.12 ± 0.26	1.97 ± 0.05	1	ox.
MET 00426	FGR	MET_01B_91	200 × 220	5.97 ± 0.30	1.88 ± 0.05	1	sil.
MET 00426	FGR	MET_01D_1	210 × 235	5.51 ± 0.72	1.22 ± 0.11	1	sil.
MET 00426	FGR	MET_01D_10	140 × 235	5.39 ± 0.46	1.62 ± 0.08	1	sil.
Acfer 094	FGR	RC#11_01_02	350 × 210	5.52 ± 0.42	1.99 ± 0.08	1	sil.
Acfer 094	FGR	RC#11_01_04	230 × 165	6.46 ± 0.46	2.02 ± 0.08	1	sil.
Acfer 094	FGR	RC#11_01_05	210 × 165	13.20 ± 1.01	2.01 ± 0.13	1	sil.
Acfer 094	FGR	RC#11_01_08	370 × 260	8.62 ± 0.67	2.11 ± 0.10	1	sil.
Acfer 094	FGR	RC#11_01_11	230 × 210	7.08 ± 0.54	2.12 ± 0.09	1	sil.
Acfer 094	FGR	RC#11_01_13	210 × 260	5.95 ± 0.46	1.79 ± 0.08	1	sil.
Acfer 094	FGR	RC#11_01_22	350 × 400	14.20 ± 1.32	2.27 ± 0.16	1	sil.
Acfer 094	FGR	RC#12_03	230 × 280	6.84 ± 0.52	1.83 ± 0.08	1	sil.
Acfer 094	FGR	RC#12_08	200 × 235	5.44 ± 0.41	1.74 ± 0.07	1	sil.

phous silicates and the presolar grain abundances (Fig. 3) of the respective rims.

3.4. Presolar grain compositions as indicators for secondary processing

It has been demonstrated previously that presolar grains can be used as "analytical tools" to assess the degree of alteration experienced by the host material (e.g., Floss and Stadermann, 2009, 2012; Leitner et al., 2012). This is true not only for the abundances and abundance ratios of different presolar grain species, but also for the elemental compositions of individual grains, which can give hints about possible aqueous or thermal alteration.

The elemental composition of 19 presolar silicates from GRA 95229 and EET 92161 were investigated by AES (Auger Electron Spectroscopy) from which (Mg + Fe)/Si and Mg/(Mg + Fe) ratios were determined (Table 4, Fig. 6). All grains are ferromagnesian silicates. The (Mg + Fe)/Si ratios follow a pattern similar to that observed for the presolar silicates in other primitive chondrites (Floss and Stadermann, 2009, 2012; Vollmer et al., 2009a; Nguyen et al., 2010; Zhao et al., 2013; Bose et al., 2010, 2012). Three grains show (Mg + Fe)/Si ratios compatible with a pyroxene-like (Px) composition, four grains have olivine-like (Ol) (Mg + Fe)/Si ratios and six silicates have intermediate compositions, with (Mg + Fe)/Si between 1 (Px) and 2 (Ol) (cf. Stadermann et al., 2009). One grain (GR95_14_13) has a (Mg + Fe)/Si significantly below 1, and an O/Si-ratio of ∼2. Mg and Fe are present in the spectrum; therefore, it is not a pure SiO_2-grain, but possibly a GEMS-like ("glass with embedded metal and sulfide") grain. Another three grains have Si-poor compositions, and two grains (GR95_13_27, GR95_13_29) display complex compositions, with differing (Mg + Fe)/Si ratios

for each of the 2–3 spectra acquired for individual sub-regions, corresponding to composite structures visible in the SEM (an example for GR95_13_29 is shown in Fig. S1). The investigated grains show Mg/(Mg+Fe) ratios ranging from 0.2 to 0.8. This is, on average, more Fe-rich than predicted by current stellar models and astronomical observations (e.g., Demyk et al., 2000) and has been observed for the presolar silicate populations in the most primitive chondrites like Acfer 094 (Vollmer et al., 2009a, 2009b; Bose et al., 2010), ALHA 77307 (Nguyen et al., 2010; Bose et al., 2012), QUE 99177 (Floss and Stadermann, 2009), MET 00426 (Floss and Stadermann, 2009), and GRV 021710 (Zhao et al., 2013). The overall compositions of the grains in the FGR and ICM materials studied here show no significant differences from what is observed in chondrites showing only very little evidence of aqueous alteration. In addition, we do not observe widespread alteration effects like alteration rims, "haloes", or fuzzy grain boundaries that would be indicative of extensive aqueous alteration (e.g. Brearley, 2006).

We also did not observe any visible effects of thermal alteration on the presolar silicates. In their study of the C2-ungrouped chondrite Adelaide, Floss and Stadermann (2012) observed "coarsening" of the matrix in more altered areas, attributed to thermal annealing of the material. Moreover, a large fraction of the studied presolar grains showed compositions that were significantly more Fe-rich than presolar silicates from other primitive chondrites, which the authors also attributed to thermal alteration effects. Clearly, the grains found in this study did not suffer such thermal alteration. Since the FGR-material was accreted onto presumably hot chondrules, this observation indicates a rapid cooling for the accreting chondrules.
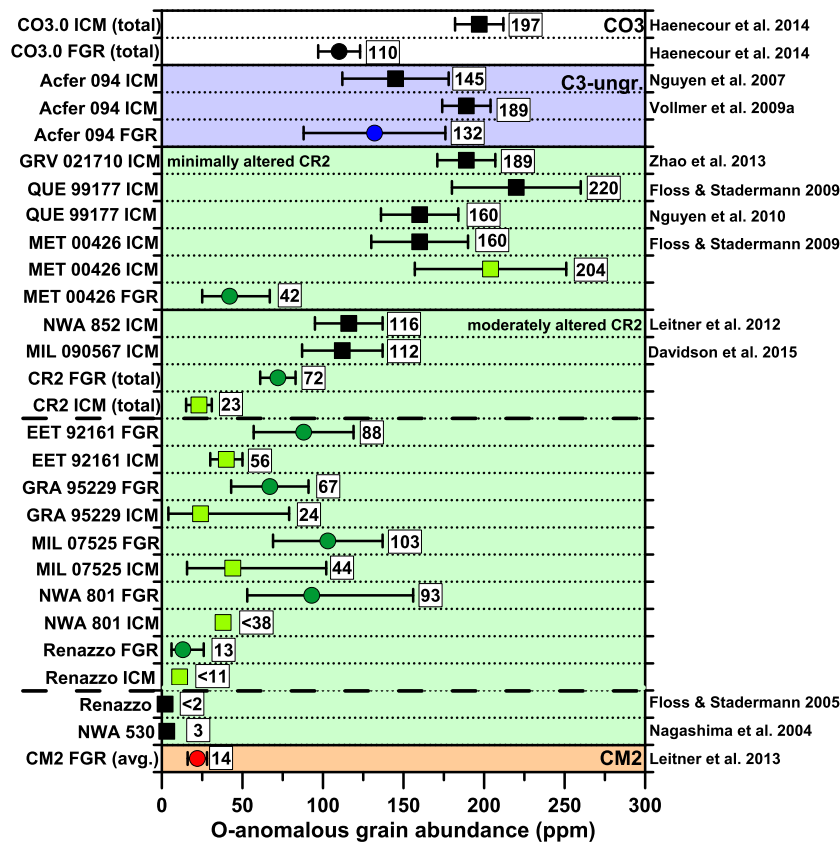
Fig. 3. Abundances (in ppm) of presolar O-rich dust grains for the CR chondrites and Acfer 094 investigated in this study (green and blue symbols) in comparison with literature data for CM, CR and CO chondrites, as well as the ungrouped carbonaceous chondrite Acfer 094. All errors are 1σ. (For interpretation of the references to color in this figure legend, the reader is referred to the web version of this article.)

3.5. Implications for rim formation and aqueous alteration of the fine-grained matter

For the FGRs investigated in this study, origin and possible formation processes can be further constrained. From the presence of presolar stardust together with the overall composition and texture of the fine-grained host material, rim formation from chondrule debris or by chondrule erosion after incorporation into a parent body can be excluded. Nebular accretion of fine-grained materials unto chondrule surfaces has been discussed by several authors (e.g., Bland et al., 2011; Ciesla et al., 2003), and recent studies (Beitz et al., 2013a, 2013b) demonstrated experimentally the feasibility of rim accretion under nebular conditions. In such "nebular accretion" scenarios, model-derived and experimentally determined rim porosities are much higher than what is observed in chondritic FGRs. Therefore, additional compaction processes must have taken place either in the nebula or on the respective parent bodies. Compaction of the fine-grained rim material on the parent body has been proposed (Trigo-Rodriguez et al., 2006); however, the fine-grained material itself was believed to have accreted onto the chondrule surface prior to parent body formation. Trigo-Rodriguez et al. (2006) invoked "collisional compaction processes within parent bodies" to explain the formation of FGRs, but other researchers (Beitz et al., 2013a, 2013b) did not observe any signs of a density increase for the rims around the chondrule analogues of their experiments, which would have been indicative for the aforementioned parent body compaction processes. It is also not made clear why such internal processes would produce sharply defined boundaries between rims as we observed in the chondritic material. Therefore, we consider this hypothesis as unlikely for the production of FGRs.

Volume filling factors might be enhanced by aqueous alteration, as suggested by Takayama and Tomeoka (2012) for rims in the Tagish Lake meteorite. This could, in theory, explain the fact that the observed porosities in meteoritic FGRs are higher than in theoretical predictions and experimental results. However, those rims are extensively altered and consist primarily of phyllosilicates, while the FGRs in the present study represent a relatively primitive mixture of anhydrous and altered phases showing no evidence for extensive aqueous modification.

Impacts have been suggested as relevant parent-body processes for the compaction of fine-grained material in the vicinity of chondrules (Bland et al., 2011); however, these processes are not considered as fundamental for the *formation* of FGRs in chondrites (Bland et al., 2011). Low-energy impacts are invoked as mechanism for compaction and lithification (Bland et al., 2012, 2014), thus preserving accretionary fabrics as observed in Allende (e.g., (Bland et al., 2011). Evidence for multiple low-intensity impacts responsible for the compaction and formation of petrofabrics has been found in CM chondrites (Lindgren et al., 2014). Such low-pressure shock events would be accompanied by fluid volatilization (Bland et al., 2012). Recent work by Bland et al. (2014) demonstrated that low-energy impacts, which would cause no shock signatures in compact meteoritic components like chondrules, can cause significant temperature increases (exceeding 1000 K in localized spots) in the adjacent fine-grained porous material. Such heating events would be short (<10 s), with the chondrules acting as heat sinks. These effects could explain (partially) our observations for the moderately to more severely altered CR2 chondrites: In the chondrite formation region in the early solar nebula, a fraction of the chondrules accreted fine-grained dust rims. These rims were (partially) disrupted and compacted by multiple collisions oc-
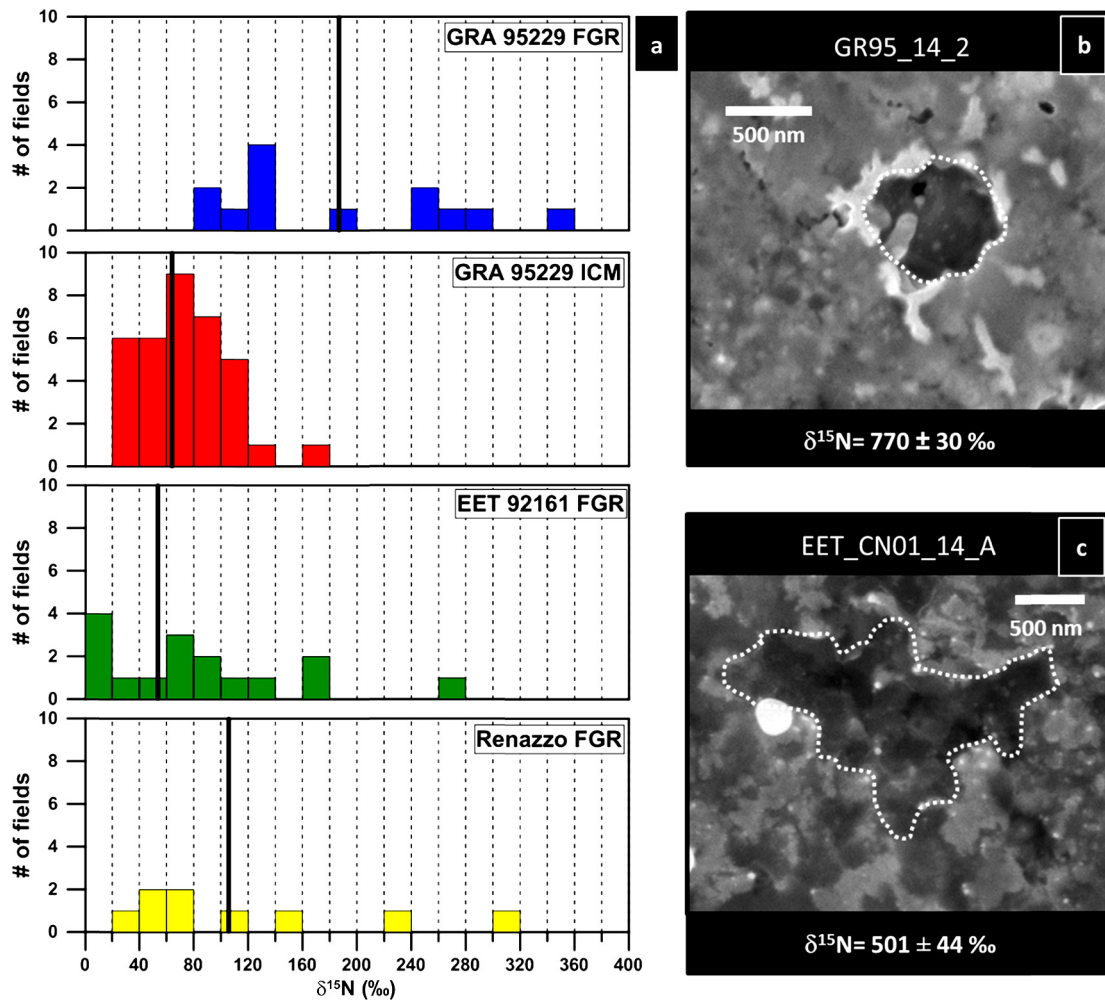
Fig. 4. (a) Nitrogen isotopic compositions of individual measurement fields (10×10 μm^2) in FGRs from GRA 95229, EET 92161, Renazzo, and in the ICM of GRA 95229. The N-isotopic compositions are displayed as δ-values, i.e., per mil deviations from the terrestrial value (^{15}N/^{14}N $= 3.676 \times 10^{-3}$). The bold lines in each plot mark the respective weighted average δ^{15}N. (b) SEM micrograph showing localized spots of organic material with anomalous N-isotopic composition (marked by the white dotted lines; data not shown in (a)) in a FGR from GRA 95229. (c) SEM micrograph showing localized spots of organic material with anomalous N-isotopic composition (marked by the white dotted lines; data not shown in (a)) in a FGR from EET 92161 are displayed. All errors are 1σ.

curring during parent body formation. After FGR accretion, the material was aqueously altered by shock-released water from accreted (water) ice grains, which lead to a reduced presolar silicate abundance compared to the fine-grained precursor material, depending on the shock energy and the amount of accreted ice. Isotopic homogenization of presolar grains on timescales of ∼0.1–10 s can be expected (Bland et al., 2012), further reducing the concentration of presolar material in the FGRs. From this reservoir of fine-grained dust, rimmed and rimless chondrules, as well as other larger constituents, chondritic parent bodies accreted. During this formation process, the fine-grained component experienced impact-induced shock heating as outlined by Bland et al. (2014), which further modified its presolar grain content.

Bland et al. (2011) find evidence from fabric analysis of matrix and fine-grained rim material in the Allende meteorite (CV3) for nebular accretion and compaction of the rim structure. They report in their study the absence of any strain to the rock fabric of a FGR, resulting in a spherically symmetric stress field. The absence of strain shadows in the rock fabric, together with the observation of the juxtaposition of a uniaxial and a spherically symmetric stress field contradict models which suggest parent body compaction processes (e.g., Tomeoka and Tanimura, 2000; Trigo-Rodriguez et al., 2006). The latter models would require multiple impacts on the parent body, which would not allow the

preservation of such spherically symmetric stress fields. Moreover, multiple impacts would preclude the recording of a uniaxial stress field caused by a singular impact event, as observed by Bland et al. (2011).

Several studies (Blum and Schräpler, 2004; Ormel et al., 2008; Dominik and Tielens, 1997) predicted high initial FGR porosities after accretion in the nebula, which is in good accordance with the estimates by Bland et al. (2011) as well as the observations by Beitz et al. (2013a, 2013b). Compaction would then occur by combinations of chondrule-dust-interactions and low-intensity shocks. Impact-induced shock heating, even at low collision velocities ($v \sim 0.75$–2 km/s), could result in bulk temperatures of ∼400–700 K in the fine-grained material (with localized spots experiencing T (peak) >1000 K), but would not be recorded in the compact chondrules, which would act as heat sinks. This would create heterogeneous structures on the sub-mm scale, as are observed in chondritic meteorites, and allow for fast cooling (<10 s) and lithification of the fine-grained material (Bland et al., 2014).

We envision the processes responsible for the observed differences in the presolar grain abundances as following:

For pristine or minimally altered carbonaceous chondrites, the very primitive ICM displays high presolar grain abundances in the range of 150 to 250 ppm (Floss and Stadermann, 2009;
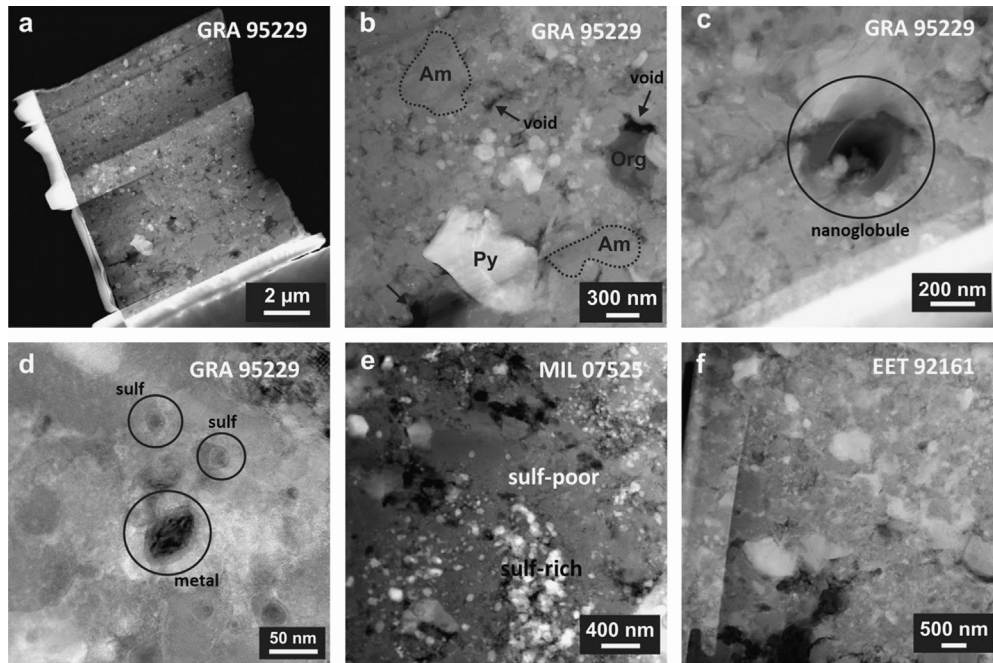
Fig. 5. TEM images of FIB lamellae from FGRs in GRA 95229, EET 92161, and MIL 07525. (a) HAADF (high-angle annular dark-field) image from GRA. (b) Close-up HAADF image from GRA with pyrrhotite (Py), organic matter (Org), amorphous silicates (Am) and voids (arrow-marked). (c) Close-up HAADF image of a hollow organic nanoglobule from GRA. (d) Close-up bright-field image with sub-micrometer-sized sulfide and metal grains exhibiting reaction rims (encircled) from GRA. (e) HAADF image of the MIL lamella with distinct sulfide-rich (bright) and -poor (dark) areas. (f) HAADF image from EET showing major signs of recrystallization (upper half) as low-porosity Fe-enriched (bright) areas.
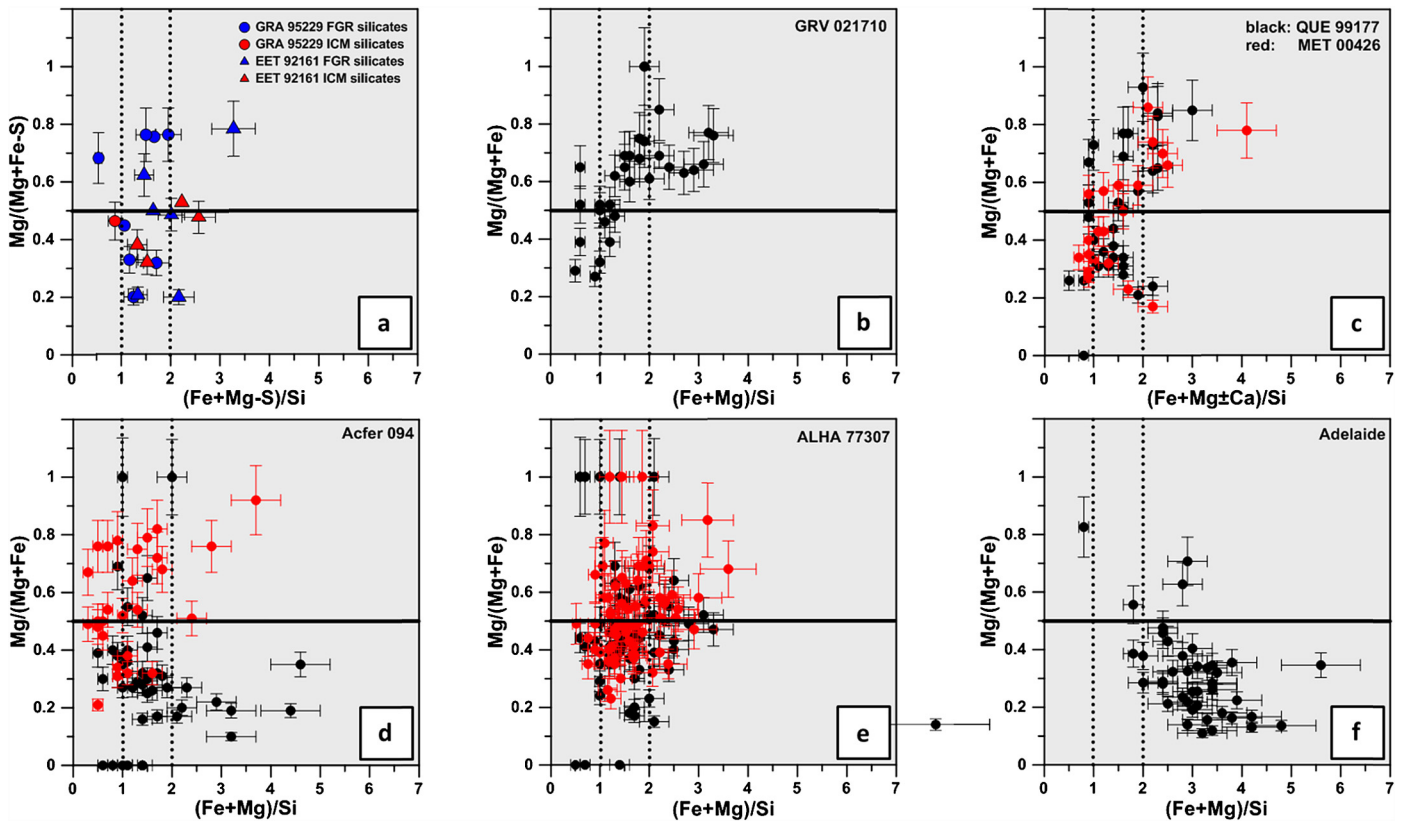
Fig. 6. (a) Mg–Fe–Si element abundances for presolar silicates from FGRs and ICM in GRA 95229 and EET 92161, (b) presolar silicate data from GRV 021710 (CR) (Zhao et al., 2013), (c) QUE 99177 and MET 00426 (both CR) (Floss and Stadermann, 2009), (d) Acfer 094 (C-ungrouped) (Vollmer et al., 2009a; Bose et al., 2010), (e) ALHA 77307 (CO3.0) (Nguyen et al., 2010; Bose et al., 2012), and Adelaide (C-ungrouped) (Floss and Stadermann, 2012) (f). All errors are 1σ. "Fe $+$ Mg $-$ S" means that the ratios have been corrected for the presence of S. Dotted vertical lines denote the compositions of stoichiometric pyroxene (1) and olivine (2). The horizontal lines mark the border between Mg-rich and Fe-rich compositions.

Table 4

Elemental compositions of presolar silicate grains from GRA 95229 and EET 92161 determined by Auger electron spectroscopy (AES). Relative abundance errors are 3.6% (O), 11.2% (Fe), 9.4% (Mg), 11% (Si), 24.9% (Al), and 10% (S). "px-like" and "ol-like" stand for pyroxene- and olivine-like grain stoichiometries ((Mg + Fe − S/Si) ∼ 1 and ∼2), respectively. "intermed." denotes grains with intermediate ratios of ∼1.3 to 1.7, while "Si-rich" and "Si-poor" characterize grains with respective ratios >2 and <1. "Compound" denotes grains that consist of sub-grains with significantly different (Mg + Fe − S)/Si and/or Mg/(Mg + Fe − S) ratios.

Grain	O	Fe	Mg	Si	Al	S	(Mg + Fe − S)/Si[a]	Mg/(Mg + Fe − S[a])	Type
GR95_4_16	59.9	18.2	3.8	15.4		2.8	1.2 ± 0.2	0.20	px-like
GR95_8_7	56.1	8.2	4.5	11.1	14.1	3.0	0.9 ± 0.1	0.46	px-like
GR95_12_5	56.8	16.7	6.2	16.2		4.0	1.2 ± 0.2	0.33	px-like
GR95_12_6	58.9	5.8	18.8	16.4			1.5 ± 0.2	0.76	intermed.
GR95_13_22	61.7	6.0	19.4	13.0			2.0 ± 0.3	0.76	ol-like
GR95_13_24	55.5	19.7	7.3	13.4		4.1	1.7 ± 0.3	0.32	ol-like
GR95_13_27	51.7	9.7	19.6	15.5		3.4	1.7 ± 0.1	0.76	compound
GR95_13_29	58.1	11.5	9.3	19.6		1.6	1.0 ± 0.1	0.45	compound
GR95_14_13	52.4	7.5	10.0	27.2		2.9	0.5 ± 0.1	0.68	Si-rich
EET_02A_B_2	55.0	7.5	27.1	10.5			3.3 ± 0.4	0.78	Si-poor
EET_02A_B_3	61.0	8.7	14.5	15.9			1.5 ± 0.2	0.62	intermed.
EET_02A_B_10	57.0	14.8	14.0	14.3			2.0 ± 0.3	0.49	ol-like
EET_02A_B_31	58.8	12.2	12.2	14.8		2.0	1.5 ± 0.2	0.50	intermed.
EET_02B_2	58.7	18.7	4.9	17.7			1.3 ± 0.2	0.21	intermed.
EET_02B_9	61.5	21.1	5.2	12.2			2.2 ± 0.3	0.20	ol-like
EET_5B_5	55.4	16.3	13.9	11.8		2.7	2.3 ± 0.2	0.50	Si-poor
EET_6_6	54.4	19.2	7.9	16.2		2.4	1.5 ± 0.2	0.32	intermed.
EET_6_13	54.4	17.4	8.0	16.0		4.2	1.3 ± 0.2	0.38	intermed.
EET_6_15	56.6	16.4	14.9	12.2			2.6 ± 0.3	0.48	Si-poor

[a] Both ratios have been corrected for the presence of S in the grains. Assuming that sulfur is present as FeS, the S abundances have been subtracted directly from the measured Fe abundances.

Vollmer et al., 2009a; Haenecour et al., 2014), while FGRs can display lower abundances (Fig. 3).

For moderately altered carbonaceous chondrites, like the majority of CR2 chondrites investigated in this study, aqueous parent body alteration has decreased the presolar silicate abundances in the respective ICM, while the FGRs were "protected" to a certain degree by their compacted nature.

In more severely altered chondrites, like Renazzo in this study, and the CM chondrites studied by Leitner et al. (2013), presolar silicate abundances in ICM and FGRs were further reduced by more extensive aqueous alteration. Due to low presolar grain statistics, it was not possible to identify differences between the abundances in FGRs and ICM for individual meteorites in many cases. Nevertheless, when we calculate the respective abundances for the total investigated ICM and FGR areas, the differences become visible (Fig. 3).

4. Conclusions

Presolar grains are circumstellar condensates that date from before the formation of our Solar System that can be found in the fine-grained component of chondritic meteorites. Our study found presolar silicate and oxide grains in several fine-grained chondrule rims of carbonaceous chondrites that experienced varying degrees of aqueous alteration, ranging from nearly pristine/minimally altered to more severely altered. Due to limited statistics, we observe differences of presolar O-rich grain abundances between fine-grained rims around chondrules (FGRs) and the interchondrule matrix (ICM) for individual meteorites only with 1-sigma significance in most of the cases (Fig. 3, Table S1). However, the "total" or combined grain abundance for the FGRs in *all* investigated samples and the respective total abundance for the ICM, differ by a factor of 3 for the moderately and more severely altered CR chondrites. For the minimally altered CR chondrite MET 00426, we observed higher abundances in the interchondrule matrices than in the fine-grained rims, and for the ungrouped carbonaceous chondrite Acfer 094, the values for ICM and FGR overlap within the error limits.

The elemental compositions of presolar silicate grains in the moderately altered CR2 chondrites GRA 95229 and EET 92161 do not differ significantly from those of presolar silicates and oxides found in the most primitive carbonaceous chondrites, i.e., no signs

for significantly higher degrees of alteration for the grains were observed. The fine-grained rims contain organic material with ^{15}N-excesses similar to what is typically observed in the matrix of CR chondrites. The N-anomalies are inherited from the protosolar nebula (e.g., Alexander et al., 2007; Busemann et al., 2006), and their presence in the FGRs further indicates a nebular origin of the rim material. Obviously, the material did not experience any alteration that would have been capable of diluting or even homogenize the anomalous isotopic signatures. TEM investigations revealed that the FGR material in the vicinity of preserved presolar grains consists of a heterogeneous mixture of pristine nebular material and components showing various degrees of aqueous alteration.

In summary, these observations indicate a nebular origin of the fine-grained material comprising the FGRs studied here. The observed differences between the total presolar silicate and oxide abundances in the fine-grained rims and the interchondrule matrix of the moderately to more severely altered CR2 chondrites and the minimally altered carbonaceous chondrites of this study imply different alteration paths for the fine-grained rims and the C2- and C3-matrix. This indicates a nebular origin of the FGRs, and incorporation by accretion for the rimmed chondrules. Furthermore, our findings clearly show that fine-grained chondrule rims like the ones investigated in this study cannot have formed by chondrule erosion or regolith gardening processes on the respective parent bodies. However, one has to keep in mind that chondritic meteorites contain various types of chondrule rims. Thus, different formation scenarios might very well apply for other rims that have been labeled "fine-grained" despite a clearly different composition or structure (e.g., Takayama and Tomeoka, 2012), and a universal rim formation process seems rather unlikely.

Appendix A. Supplementary material

Supplementary material related to this article can be found online at http://dx.doi.org/10.1016/j.epsl.2015.11.028.

References

Abreu, N.M., Brearley, A.J., 2010. Early solar system processes recorded in the matrices of two highly pristine CR3 carbonaceous chondrites, MET 00426 and QUE 99177. Geochim. Cosmochim. Acta 74, 1146–1171.

Alexander, C.M.O'D., Fogel, M., Yabuta, H., Cody, G.D., 2007. The origin and evolution of chondrites recorded in the elemental and isotopic compositions of their macromolecular organic matter. Geochim. Cosmochim. Acta 71, 4380–4403.

Alexander, C.M.O'D., Howard, K.T., Bowden, R., Fogel, M.L., 2013. The classification of CM and CR chondrites using bulk H, C and N abundances and isotopic compositions. Geochim. Cosmochim. Acta 123, 244–260.

Allen, J.S., Nozette, S., Wilkening, L.L., 1980. A study of chondrule rims and chondrule irradiation records in unequilibrated ordinary chondrites. Geochim. Cosmochim. Acta 44, 1161–1175.

Beitz, E., Güttler, C., Nakamura, A.M., Tsuchiyama, A., Blum, J., 2013a. Experiments on the consolidation of chondrules and the formation of dense rims around chondrules. Icarus 225, 558–569.

Beitz, E., Blum, J., Mathieu, R., Pack, A., Hezel, D., 2013b. Experimental investigation of the nebular formation of chondrule rims and the formation of chondrite parent bodies. Geochim. Cosmochim. Acta 116, 41–51.

Bland, P.A., Stadermann, F.J., Floss, C., Rost, D., Vicenzi, E.P., Kearsley, A.T., Benedix, G.K., 2007. A cornucopia of presolar and early solar system materials at the micrometer size range in primitive chondrite matrix. Meteorit. Planet. Sci. 42, 1417–1427.

Bland, P.A., Howard, L.E., Prior, D.J., Wheeler, J., Hough, R.M., Dyl, K.A., 2011. Earliest rock fabric formed in the Solar System preserved in a chondrule rim. Nat. Geosci. 4, 244–247.

Bland, P.A., Muxworthy, A.R., Collins, G.S., Moore, J., Davison, T.M., Prior, D.J., Wheeler, J., Ciesla, F.J., Dyl, K.A., 2012. Effect of low intensity impacts on chondrite matrix. In: Mackwell, S.J. (Ed.), Lunar Planet. Sci. Conf., vol. 43. LPI, Houston, TX. 2005.

Bland, P.A., Collins, G.S., Davison, T.M., Abreu, N.M., Ciesla, F.J., Muxworthy, A.R., Moore, J., 2014. Pressure–temperature evolution of primordial solar system solids during impact-induced compaction. Nat. Commun. 5, 5451–5463. http://dx.doi.org/10.1038/ncomms6451.

Blum, J., Schräpler, R., 2004. Structure and mechanical properties of high-porosity macroscopic agglomerates formed by random ballistic deposition. Phys. Rev. Lett. 93, 115503.

Bose, M., Floss, C., Stadermann, F.J., 2010. An investigation into the origin of Fe-rich presolar silicates in Acfer 094. Astrophys. J. 714, 1624–1636.

Bose, M., Floss, C., Stadermann, F.J., Stroud, R.M., Speck, A.K., 2012. Circumstellar and interstellar material in the CO3 chondrite ALHA77307: an isotopic and elemental investigation. Geochim. Cosmochim. Acta 93, 77–101.

Brearley, A.J., 1993. Matrix and fine-grained rims in the unequilibrated CO3 chondrite, ALHA 77307: origins and evidence for diverse, primitive nebular dust components. Geochim. Cosmochim. Acta 57, 1521–1550.

Brearley, A.J., 2006. The action of water. In: Lauretta, D.S., McSween Jr., H.Y. (Eds.), Meteorites and the Early Solar System II. University of Arizona Press, Tucson, pp. 584–624. 943 pp.

Busemann, H., Young, A.F., Alexander, C.M.O'D., Hoppe, P., Mukhopadhyay, S., Nittler, L.R., 2006. Interstellar chemistry recorded in organic matter from primitive meteorites. Science 312, 727–730.

Chizmadia, L.J., Brearley, A.J., 2008. Mineralogy, aqueous alteration, and primitive textural characteristics of fine-grained rims in the Y-791198 CM2 carbonaceous chondrite: TEM observations and comparison to ALHA81002. Geochim. Cosmochim. Acta 72, 602–625.

Choi, B.-G., Huss, G.R., Wasserburg, G.J., Gallino, R., 1998. Presolar corundum and spinel in ordinary chondrites: origins from AGB stars and a supernova. Science 282, 1284–1289.

Ciesla, F.J., Lauretta, D.S., Cohen, B.A., Hood, L.L., 2003. A nebular origin for chondritic fine-grained phyllosilicates. Science 299, 549.

Davidson, J., 2009. NanoSIMS and beyond: presolar grains in primitive materials and Solar System formation. Ph.D. dissertation. Open University, Milton Keynes, UK.

Davidson, J., Busemann, H., Franchi, I.A., 2012. Presolar grain inventory of a fine-grained rim in the CO3.0 ALHA 77307. Meteorit. Planet. Sci. Suppl. Abstract #5269.

Davidson, J., Busemann, H., Nittler, L.R., Alexander, C.M.O'D., Orthous-Daunay, F.-R., Franchi, I.A., Hoppe, P., 2014. Abundances of presolar silicon carbide grains in primitive meteorites determined by NanoSIMS. Geochim. Cosmochim. Acta 139, 248–266.

Davidson, J., Alexander, C.M.O'D., Schrader, D.L., Nittler, L.R., Bowden, R., 2015. Miller Range 090657: a very pristine Renazzo-like (CR) Carbonaceous Chondrite. In: Mackwell, S.J. (Ed.), Lunar Planet Sci. Conf., vol. 44. LPI, Houston, TX.

Demyk, K., Dartois, E., Wiesemeyer, H., Jones, A.P., d'Hendecourt, L., 2000. Structure and chemical composition of the silicate dust around OH/IR stars. Astron. Astrophys. 364, 170–178.

Dominik, C., Tielens, A.G.G.M., 1997. The physics of dust coagulation and the structure of dust aggregates in space. Astrophys. J. 480, 647–673.

Floss, C., Stadermann, F.J., 2005. Presolar (circumstellar and interstellar) phases in Renazzo: the effects of parent body processing. In: Mackwell, S.J. (Ed.), Lunar Planet Sci. Conf., vol. 36. LPI, Houston, TX. 1390.

Floss, C., Stadermann, F.J., 2009. Auger Nanoprobe analysis of presolar ferromagnesian silicate grains from primitive CR chondrites QUE 99177 and MET 00426. Geochim. Cosmochim. Acta 73, 2415–2440.

Floss, C., Stadermann, F.J., 2012. Presolar silicate and oxide abundances and compositions in the ungrouped carbonaceous chondrite Adelaide and the K chondrite Kakangari: the effects of secondary processing. Meteorit. Planet. Sci. 47, 992–1009.

Gehrels, N., 1986. Confidence limits for small numbers of events in astrophysical data. Astrophys. J. 303, 336–346.

Haenecour, P., Floss, C., 2012. Stardust in fine-grained chondrule rims and matrix in LaPaz 031117: insights into the conditions of dust accretion in the Solar Nebula. In: Mackwell, S.J. (Ed.), Lunar Planet. Sci. Conf., vol. 43. LPI, Houston, TX. 1659.

Haenecour, P., Floss, C., Joliff, B.L., Zega, T.J., Bose, M., Carpenter, P., 2014. Presolar silicates as tracers of the formation of fine-grained chondrule rims in CO3 chondrites. In: Mackwell, S.J. (Ed.), Lunar Planet. Sci. Conf., vol. 45. LPI, Houston, TX. 1316.

Harju, E.R., Rubin, A.E., Ahn, I., Choi, B.-G., Ziegler, K., Wasson, J.T., 2014. Progressive aqueous alteration of CR carbonaceous chondrites. Geochim. Cosmochim. Acta 139, 267–292.

Howard, K.T., Alexander, C.M.O'D., Schrader, D.L., Dyl, K.A., 2015. Modal mineralogy of CM2 chondrites by X-ray diffraction (PSD-XRD). Part 1: Total phyllosilicate abundance and the degree of aqueous alteration. Geochim. Cosmochim. Acta 149, 206–222.

Huss, G.R., Meshik, A.P., Smith, J.B., Hohenberg, C.M., 2003. Presolar diamond, silicon carbide, and graphite in carbonaceous chondrites: implications for thermal processing in the solar nebula. Geochim. Cosmochim. Acta 67, 4823–4848.

Krot, A.N., Meibom, A., Weisberg, M.K., Keil, K., 2002. The CR chondrite clan: implications for early solar system processes. Meteorit. Planet. Sci. 37, 1451–1490.

Le Guillou, C., Brearley, A., 2014. Relationships between organics, water and early stages of aqueous alteration in the pristine CR3.0 chondrite MET 00426. Geochim. Cosmochim. Acta 131, 344–367.

Leitner, J., Vollmer, C., Hoppe, P., Zipfel, J., 2012. Characterization of presolar material in the CR chondrite Northwest Africa 852. Astrophys. J. 745, 38–53.

Leitner, J., Metzler, K., Vollmer, C., Hoppe, P., 2013. Search for presolar grains in fine-grained chondrule rims: first results from CM chondrites and Acfer 094. In: Mackwell, S.J. (Ed.), Lunar Planet. Sci. Conf., vol. 44. LPI, Houston, TX. 2273.

Lindgren, P., Hanna, R.D., Dobson, K.J., Tomkinson, T., Lee, M.R., 2014. The paradox between low shock-stage and evidence for compaction in CM carbonaceous chondrites explained by multiple low-intensity impacts. Geochim. Cosmochim. Acta 148, 159–178.

Metzler, K., Bischoff, A., Stöffler, D., 1992. Accretionary dust mantles in CM chondrites: evidence for solar nebula processes. Geochim. Cosmochim. Acta 56, 2873–2897.

Mostefaoui, S., Hoppe, P., 2004. Discovery of abundant in situ silicate and spinel grains from red giant stars in a primitive meteorite. Astrophys. J. 613, L149–L152.

Nagashima, K., Krot, A.N., Yurimoto, H., 2004. Stardust silicates from primitive meteorites. Nature 428, 921–924.

Newton, J., Bischoff, A., Arden, J.W., Franchi, I.A., Geiger, T., Greshake, A., Pillinger, C.T., 1995. Acfer 094, a uniquely primitive carbonaceous chondrite from the Sahara. Meteoritics 30, 47–56.

Nguyen, A., Stadermann, F.J., Zinner, E., Stroud, R.M., Alexander, C.M.O.D., Nittler, L.R., 2007. Characterization of presolar silicate and oxide grains in primitive carbonaceous chondrites. Astrophys. J. 656, 1223–1240.

Nguyen, A.N., Nittler, L.R., Stadermann, F.J., Stroud, R.M., Alexander, C.M.O'D, 2010. Coordinated analyses of presolar grains in the Allan Hills 77307 and Queen Elizabeth Range 99177 meteorites. Astrophys. J. 719, 166–189.

Nittler, L.R., Alexander, C.M.O'D., Gao, X., Walker, R.M., Zinner, E., 1997. Stellar sapphires: the properties and origins of presolar Al_2O_3 in meteorites. Astrophys. J. 483, 475–495.

Nittler, L.R., Alexander, C.M.O'D., Gallino, R., Hoppe, P., Nguyen, A.N., Stadermann, F.J., Zinner, E., 2008. Aluminum-, Calcium- and Titanium-rich oxide stardust in ordinary chondrite meteorites. Astrophys. J. 682, 1450–1478.

Nittler, L.R., Alexander, C.M.O'D., Stroud, R.M., 2013. High abundance of presolar materials in CO3 chondrite Dominion Range 08006. In: Mackwell, S.J. (Ed.), Lunar Planet Sci. Conf., vol. 44. LPI, Houston, TX. #2367.

Ormel, C.W., Cuzzi, J.N., Tielens, A.G.G.M., 2008. Co-accretion of chondrules and dust in the Solar nebula. Astrophys. J. 679, 1588–1610.

Schrader, D.L., Davidson, J., Greenwood, R.C., Franchi, I.A., Gibson, J.M., 2014. A water–ice rich minor body from the early Solar System: the CR chondrite parent asteroid. Earth Planet. Sci. Lett. 407, 48–60.

Scott, E.R.D., Keil, K., Stöffler, D., 1992. Shock metamorphism of carbonaceous chondrites. Geochim. Cosmochim. Acta 56, 4281–4293.

Sears, D.W.G., Benoit, P.H., Jie, L., 1993. Two chondrule groups each with distinctive rims in Murchison recognized by cathodoluminescence. Meteoritics 28, 669–675.

Stadermann, F.J., Floss, C., Bose, M., Lea, A.S., 2009. The use of Auger spectroscopy for the in situ elemental characterization of sub-micrometer presolar grains. Meteorit. Planet. Sci. 44, 1033–1049.

Takayama, A., Tomeoka, K., 2012. Fine-grained rims surrounding chondrules in the Tagish Lake carbonaceous chondrite: verification of their formation through parent-body processes. Geochim. Cosmochim. Acta 98, 1–18.

Tomeoka, K., Tanimura, I., 2000. Phyllosilicate-rich chondrule rims in the Vigarano CV3 chondrite: evidence for parent-body processes. Geochim. Cosmochim. Acta 64, 1971–1988.

Trigo-Rodriguez, J.M., Rubin, A.E., Wasson, J.T., 2006. Non-nebular origin of dark mantles around chondrules and inclusions in CM chondrites. Geochim. Cosmochim. Acta 70, 1271–1290.

Vollmer, C., Hoppe, P., Stadermann, F.J., Floss, C., Brenker, F., 2009a. NanoSIMS analysis and Auger electron spectroscopy of silicate and oxide stardust from the carbonaceous chondrite Acfer 094. Geochim. Cosmochim. Acta 73, 7127–7149.

Vollmer, C., Brenker, F., Hoppe, P., Stroud, R.M., 2009b. Direct laboratory analysis of silicate stardust from red giant stars. Astrophys. J. 700, 774–782.

Wirth, R., 2004. Focused Ion Beam (FIB): a novel technology for advanced application of micro- and nanoanalysis in geosciences and applied mineralogy. Eur. J. Mineral. 16, 863–876.

Zega, T.J., Nittler, L.R., Busemann, H., Hoppe, P., Stroud, R.M., 2007. Coordinated isotopic and mineralogic analyses of planetary materials enabled by in situ lift-out with a focused ion beam scanning electron microscope. Meteorit. Planet. Sci. 42, 1373–1386.

Zhao, X., Floss, C., Lin, Y., Bose, M., 2013. Stardust investigation into the CR chondrite Grove Mountain 021710. Astrophys. J. 769, 49.

Zinner, E., 2014. Presolar grains. In: Davis, A.M. (Ed.), Meteorites and Cosmochemical Processes. Elsevier, Amsterdam, pp. 181–213.

Zinner, E., Amari, S., Guinness, R., Nguyen, A., Stadermann, F.J., Walker, R.M., Lewis, R.S., 2003. Presolar spinel grains from the Murray and Murchison carbonaceous chondrites. Geochim. Cosmochim. Acta 67, 5083–5095.